

Article

## Mapping Spatial Patterns of *Posidonia oceanica* Meadows by Means of Daedalus ATM Airborne Sensor in the Coastal Area of Civitavecchia (Central Tyrrhenian Sea, Italy)

Flavio Borfecchia <sup>1,\*</sup>, Carla Micheli <sup>2</sup>, Filippo Carli <sup>3</sup>, Selvaggia Cognetti De Martis <sup>3</sup>,  
Valentina Gnisci <sup>3</sup>, Viviana Piermattei <sup>3</sup>, Alessandro Belmonte <sup>2</sup>, Luigi De Cecco <sup>1</sup>,  
Sandro Martini <sup>1</sup> and Marco Marcelli <sup>3</sup>

<sup>1</sup> UTMEA-TER Energy and Environment Modeling, Earth Observation and Analysis Laboratory, Casaccia Research Centre, Italian National Agency for New Technology, Energy and Sustainable Economic Development (ENEA), via Anguillarese, 301, I-00123 Rome, Italy; E-Mails: luigi.dececco@enea.it (L.C.); sandro.martini@enea.it (S.M.)

<sup>2</sup> UTRINN-BIO Renewables Energies, Biomass and Bio-Energies Laboratory, Casaccia Research Centre, ENEA, via Anguillarese, 301, I-00123 Rome, Italy; E-Mails: carla.micheli@enea.it (C.M.); ales@gmail.com (B.A.)

<sup>3</sup> Laboratory of Experimental Oceanology and Marine Ecology, Department of Biological and Ecological Sciences (DEB), La Tuscia University, molo Vespucci, Porto di Civitavecchia, I-00053 Civitavecchia (RM), Italy; E-Mails: selvaggiacdm@unitus.it; fmcarli@unitus.it (F.C.); s.cognetti@unitus.it (S.C.M.); vale.gnisci@unitus.it (V.G.); v.piermattei@unitus.it (V.P.); marcomarcell@unitus.it (M.M.)

\* Author to whom correspondence should be addressed; E-Mail: flavio.borfecchia@enea.it; Tel.: +39-6-3048-6042; Fax: +39-6-3048-3362.

Received: 2 August 2013; in revised form: 20 September 2013 / Accepted: 23 September 2013 /

Published: 8 October 2013

---

**Abstract:** The spatial distribution of sea bed covers and seagrass in coastal waters is of key importance in monitoring and managing Mediterranean shallow water environments often subject to both increasing anthropogenic impacts and climate change effects. In this context we present a methodology for effective monitoring and mapping of *Posidonia oceanica* (PO) meadows in turbid waters using remote sensing techniques tested by means of LAI (Leaf Area Index) point sea truth measurements. Preliminary results using Daedalus airborne sensor are reported referring to the PO meadows at Civitavecchia site (central Tyrrhenian sea) where vessel traffic due to presence of important harbors and huge power plant represent strong impact factors. This coastal area, 100 km far from Rome

(Central Italy), is characterized also by significant hydrodynamic variations and other anthropogenic factors that affect the health of seagrass meadows with frequent turbidity and suspended sediments in the water column. During 2011–2012 years point measurements of several parameters related to PO meadows phenology were acquired on various stations distributed along 20 km of coast between the Civitavecchia and S. Marinella sites. The Daedalus airborne sensor multispectral data were preprocessed with the support of satellite (MERIS) derived water quality parameters to obtain here improved thematic maps of the local PO distribution. Their thematic accuracy was then evaluated as agreement ( $R^2$ ) with the point sea truth measurements and regressive modeling using an on purpose developd method.

**Keywords:** *Posidonia oceanica* mapping; Daedalus ATM; airborne passive HR multispectral remote sensing; sea coastal ecosystems monitoring; LAI (Leaf Area Index); water column and atmospheric image based corrections; Multi-resolution satellite/airborne sensors integration; Landsat ETM+; MERIS Coastcolour; thematic accuracy

---

## 1. Introduction

*Posidonia oceanica* (L) Delile (PO) is one of the most important Mediterranean seagrass and is distributed along many Italian coasts which currently host more than 40% of European PO meadows. While PO ecosystems guarantee stability of the littoral zones affected by erosion and play a fundamental ecological role by providing indispensables oxygen and biomass from their photosynthetic activity to other sea organisms, here they are threatened and under stress from many factors and generally exhibit a meadows surface and productivity reduction [1]. Both the direct disturbances arising from marine activities (harborages, dredging and escavation works, ...) and the shallow waters turbidity coming from increased human factors (urban settlement concentration, agriculture, land use, ...) focusing on the coastal areas and the consequent rise of sediment and pollution discharged by the rivers are within the main reasons for Mediterranean and Italian PO decline [2]. In perspective these effects may be further strengthened by rain intensity, sea temperature and acidification rise expected by ongoing global climate changes.

Due to impacts from these different factors PO may exhibit various kind of responses to stress [2], mainly evidenced by extents reduction, fragmentation increase and changes of phenology and morphological parameters of the meadows [3]. In general the extensive analysis of such variability, by means of remote sensing monitoring and advanced laboratory analysis techniques, aims at the detection and better characterization of PO meadows specific biophysical parameters (*i.e.*, LAI) and distribution to assess their health and resilience capability [3] and possibly identify the various environmental stress factors with the perspective to better support their sustatinable management [4]. Although many biological tests have been carried out on PO as good indicator of water quality and status of marine ecosystems [4,5], its accurate spatial patterns mapping is still in progress in various Italian coastal zones affected by high anthropogenic pressure and often characterized by diffused shallow waters turbidity which often makes difficult their extensive detection by means of remote sensing techniques.

Today Earth Observation (EO) passive remote sensing techniques are widely exploited, to collect extensive data about the oceans' surface environments at different spatial and temporal scales, using mainly visible spectral radiometry, commonly known as ocean color. In fact they are able to provide effective means for synoptic studies of the marine ecosystems, whether these concerned with the open ocean or, more particularly with coastal ecosystems where processes tend to operate with higher frequency and shorter spatial scale than offshore. In spite of their usefulness for open seas studies, due to more stringent spatial scale requirements and frequent higher optical complexity (Case 2 waters) of shallow waters, such widely used remotely sensed data is unluckily less exploitable for the analysis of PO and seagrass coastal ecosystems in terms of discrimination, extension and other specific biophysical and water quality parameters.

The spatial distribution assessment of submerged vegetation in shallow sea waters is difficult and expensive to achieve, depending also on its extent. The traditional techniques based on marine surveys by means of SCUBA diving, support ships and specific tools may provide information over limited areas but are unsuitable for extensive characterization of larger coastal regions, which usually could involve prohibitive costs and resources which are not often available. To enhance the current methods, sea truth measurements should be coupled with information more suitable in terms of spatio-temporal scales and extents, as those that may be provided by the currently available earth observation (EO) polar satellite [6,7] and airborne HR/VHR (High/Very High Resolution) multispectral [8] sensors. In particular the synergic exploitation of the finer resolution and frequent, flexible over flights capability offered by airborne sensors can be more effective [9] for monitoring and mapping [10] the spatially complexes coastal ecosystems and processes in presence also of high spatio-temporal variability in water turbidity. These EO systems and particularly those based on airborne platform may provide improved capabilities even in those Northern Mediterranean coasts where the water transparency conditions are not always enough favorable to allow suitable remote sensing observations of seagrass meadows depending on the effective preprocessing capability for atmospheric and water column noise removal. In particular this former should be based on the water transparency distribution to properly account for its spatially variable effects. Although the HR remote sensing techniques have been widely used for seagrass [11,12] and sea bed covers mapping in the transparent shallow waters, very few works dealt with such applications in turbid waters where effective radiometric corrections must be implemented in order to reduce both atmosphere and water column noise contributions to recover the useful reflectance signals from the sea bottom.

In this context the main goal of this work is the implementation and test of an integrated operative methodology based on airborne remote sensing techniques for extensive thematic mapping of PO meadows coupled with their biometry in the coastal shallow waters of Civitavecchia, often affected by low transparency conditions and whose bathymetry ranges between 1 and 20 m. In order to allow an effective monitoring the requirements included a radiometric preprocessing procedure able to ensure a reduction of possible noises effects arising from water column and atmosphere turbidity. The sea truth preliminaries data, acquired within a still ongoing campaign in coastal areas near Civitavecchia town, were exploited to suitably support the methodology development and test. These sea truth point data measurements, even few, are located in correspondence of the two main local harbors and zones where different impact factors show maximum concentrations with frequent sea water low transparency conditions. In these coastal areas of the middle Italy, different anthropogenic stresses have

considerably increased in the last decades, due to the rise in fishing [13] and tourism activities and the regular sea traffic from local harbors connecting the Italian main islands (Sardinia, Sicily) and providing fuel to the local important thermo-electric power plant.

Thus the implemented methodology described in the next sections focused mainly on an original approach for the radiometric preprocessing of the Daedalus airborne remotely sensed HR data using other spectrally compatibles satellite derived EO products. In particular the local distribution of coastal water transparency parameters derived from the MERIS sensor data in the framework of the ESA (European Space Agency) Coastcolour project, was used for water column correction by means of the image-based Lyzenga method (see next chapters). The effectiveness of the implemented transparency noise removal procedure was then tested through the two thematic maps of PO distribution obtained from a spectral classification procedure of Daedalus ATM data preprocessed at different levels (with and without water column correction). The accuracy level of two thematic maps was thus assessed in term of agreement (correlation) with sea truth measured data by means of an on purpose developed method to make categorical areal data of PO thematic distribution compatible with the point measurements.

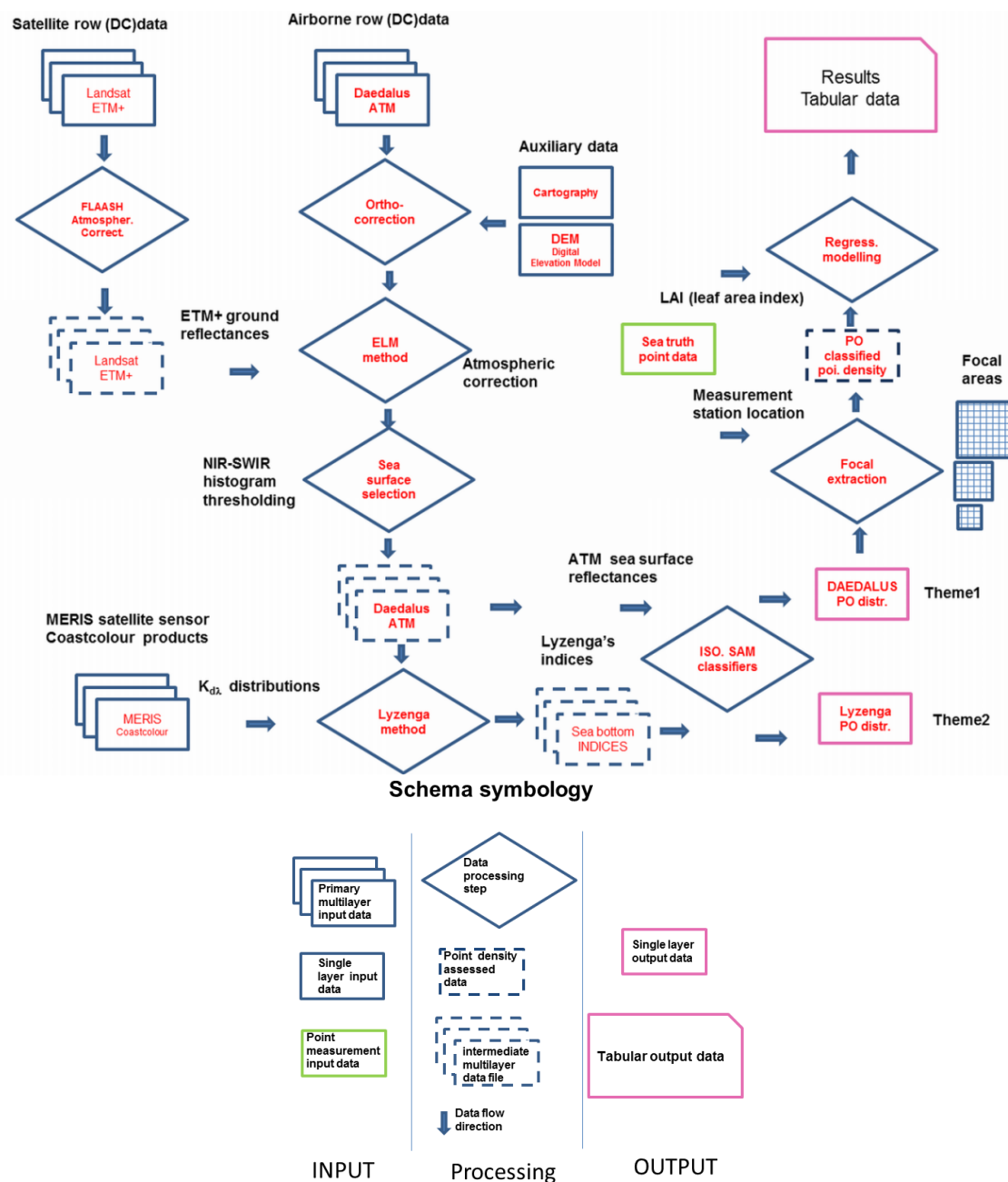
## 2. Materials and Methods

### 2.1. Implemented Methodology

Aiming at implementing an improved method able to find out more about the distribution of PO in more threatened areas and turbid waters and detect its spatial patterns mainly linked to local impact intensity and processes at various scales and according to previous works [14,15], we proposed an integrated approach based on airborne remote sensing HR observations, their suitable operative atmospheric and water column radiometric preprocessing then *in situ* validation and test. The 12 band visible (Red, Green, Blue), NIR-SWIR (Near Infrared, middle Short Wave Infra Red) and TIR (Thermal Infrared) data acquired by Daedalus 1268E sensor, were used here for methodology implementation and to derive the required thematic products while compatible Landsat ETM+ multispectral data and MERIS Coastcolour [16] products were exploited in the necessary radiometric preprocessing step to account for the atmospheric and water column noise contributions. In particular, as indicated in the following schema (Figure 1) ground reflectances retrieved from a 7 bands, Landsat ETM+ (Enhanced Thematic Mapper+) frame using a FLAASH code and ELM (Empirical Line Method) method were the main components of the atmospheric correction procedure, while the water column transparency correction was mainly based on MERIS (MEdium REsolution Imaging Spectrometer) sensor Coastcolour data products, devoted to coastal monitoring applications, and Lyzenga method. According to the attached symbology legend the Figure 1 schema describes the implemented methodology in terms of multilayer (mainly remotely sensed), single layer and point data inputs, processing steps (including methods citations referenced in the next chapters), and the main outputs, in particular the two single layer thematic maps (Theme1, Theme2) derived from classification. The auxiliary data encompassing the DEM (Digital Elevation Model) and cartographic maps at suitable scale have been used mainly for geometric correction and georeferencing purpose. In particular the Landsat ETM+ and Daedalus ATM raw data were preliminarily orthorectified and reprojected to the same UTM zone 33N (WGS84) cartographic coordinates system compatible with

that of the other used layers. The sea surface selection step reported here consisted in the subset from the entire atmospherically corrected Daedalus ATM strip of the portion related to the sea surface using the histogram thresholding of the NIR-SWIR bands, characterized by low values of water reflectances. This water surface selection step was introduced to improve the subsequent classification procedures. The Coastcolour products have been specifically designed and tested taking into account the specific monitoring needs of coastal marine applications dealing mainly with case 2 waters and turbidities arising from consistent concentrations of optically active components.

**Figure 1.** Implemented methodology scheme describing the input/output data and processing steps according to symbology explained in the following legend.



The ground resolution of 2.5 m of the acquired Daedalus ATM 1268E multispectral data were in agreement with the requirements previously defined for PO meadows effective monitoring and

mapping [17]; at the same time, thanks to its 12 bit radiometry dynamic coupled with S-Bend and roll automatic correction capability this airborne EO system is able to provide a valuable tool to be used in this particular context of shallow water sea bed monitoring. Due to operational and logistic constraints the preprocessing methodology was implemented through an “image based” approach [18] for atmospheric [19] and water column radiometric enhancement to reduce the atmospheric and water transparency noise effects typical of this middle Mediterranean coast. The preliminary sea truth measurements, acquired within our areas of interest in the framework of a still ongoing campaign for entire Tyrrhenian coast PO monitoring, were preliminarily used here for calibration and testing purposes. The compatibility between satellite EO products and Daedalus ATM data was assumed from acquisition date and spectral features and then preliminary checked by manual and photointerpretation procedures. As you can see the main outputs consist in two thematic maps of PO distribution obtained respectively from atmospherically corrected (Theme1) and from atmospherically plus water column corrected (Theme2) Daedalus ATM data, while tabular data refers to their agreement assessment on the basis of sea truth measurements.

## 2.2. Area of Interest

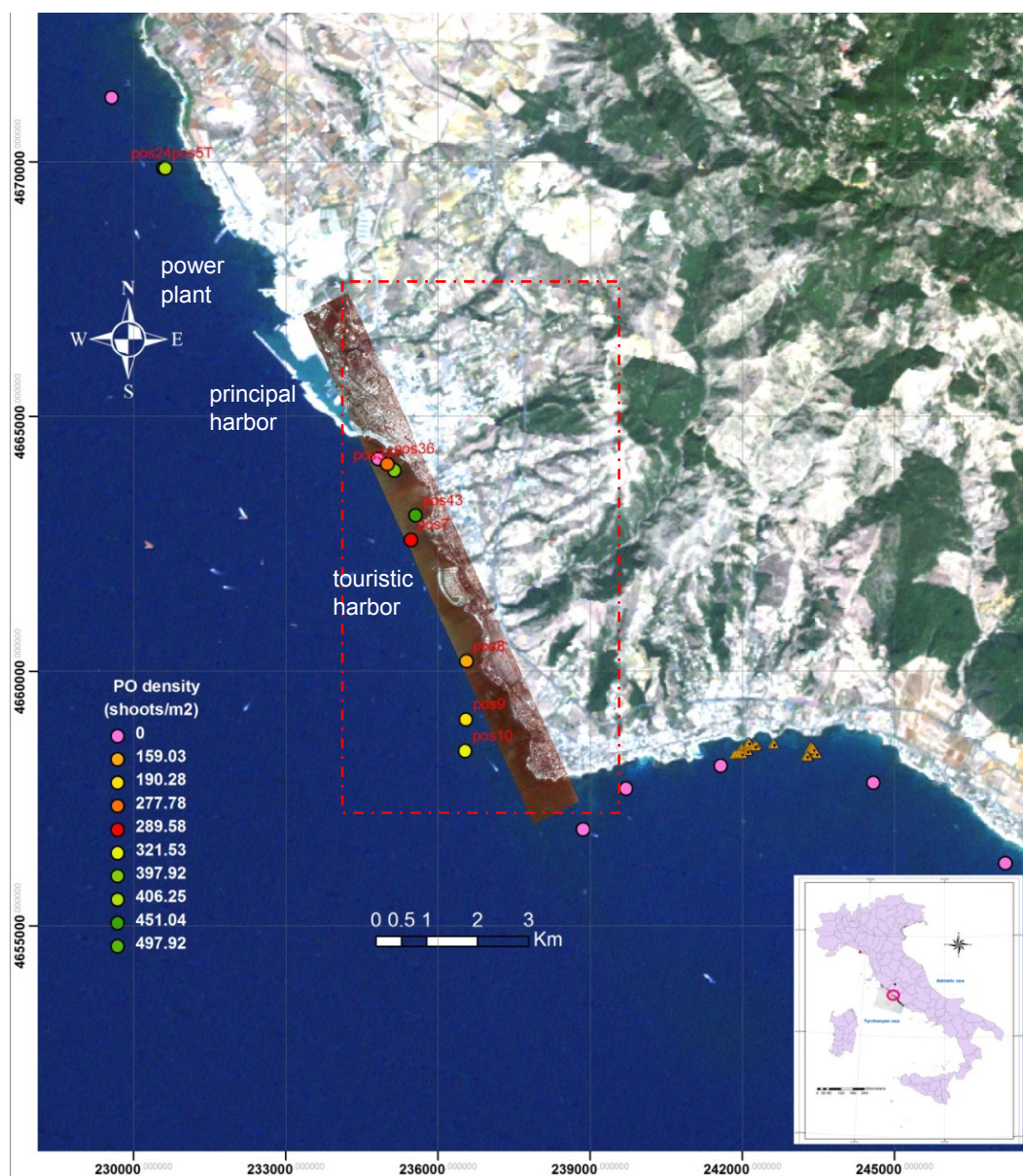
The Tyrrhenian coastal areas of Civitavecchia (Rome, Italy) is particularly complex from both a socio-economic and an ecological point of view since it hosts several economically relevant activities relating to tourism, power industry, agriculture, fisheries, aquaculture and cultural heritage with important monuments and infrastructures (harbours, dykes, *etc.*) which feature the territory. From an environmental point of view, the study area is characterized by various minor streams with seasonal regime that often can bring suspended matter with natural and anthropic pollutant, by a very complex ground's morphology affecting the wind regimes and coastal currents.

The presence of important benthic biocenosis (such as PO meadows) which are particularly sensitive to climate changes and suffer not only for seasonal sharp variations of current hydrodynamic field but also for the effects of local harbour (dredging, vessel traffic, *etc.*), and other anthropogenic activities threatening the coastal ecosystems, requires effective and integrated monitoring programs at suitable spatio-temporal scales as those that may be obtained through remote sensing techniques coupled with *in situ* calibration measurements. Figure 2 shows a true colors synoptic view of our coastal area of interest in the middle Tyrrhenian sea as acquired by ETM+ Landsat satellite polar sensor on 2 October 2011 to which the Daedalus ATM 1268E strip (acquired on 23 October 2011) was superimposed. Here the PO sea truth sampling stations are reported as colored circular symbols. Their filling color represents the categories of measured PO densities in terms of n. shoots/m<sup>2</sup>, while the station to be completed are reported in violet color. As stated before the present work focused on the coastal area near Civitavecchia (within the dashed red contours box on Figure 2) town while a previous project [20] has dealt with the seagrass mapping in the contiguous more southern areas of S. Marinella using the Quick-Bird data acquired on 21 April 2010. Here a PO restoration pilot intervention (triangular yellows symbols) through a transplantation innovative methods was carried out to account for PO meadow damages during dredging works, near Civitavecchia port. Continuing that activity the main goal of the present work was the methods implementation for detecting and monitoring the contiguous PO meadows, in the Civitavecchia coast, especially near the more threatened areas close to



the harbors. In the monitored coastal areas different impact factors arising mainly from anthropogenic activities concentration linked mainly with harbors and power plant presence are threatening the PO meadows, in particular their damages from ships frequent berth and harborages have reduced the meadows extent in correspondence of main harbors. In addition the pollutants, nutrients and sediments load coming from urban coastal settlements, agricultural practices and local rivers discharge often reduce the water transparency with further impacts on the local PO ecosystems.

**Figure 2.** Landsat ETM+ true color synoptic image of the coastal Tyrrhenian area of interest. The georeferenced strip of Daedalus ATM 1268E is superimposed both with PO sampling stations as circular symbols. The violet ones (reported with 0 density in legend) refer to the sampling stations which have been only localized and whose measurements are ongoing. The synoptic image in lower right corner depicts the area of interest as unfilled red circle in the middle Italy, in overlay to MERIS false color  $k_d$  image subset. The yellow triangles symbols are located in correspondence of the near S. Marinella areas of interest. Cartographic Projection: UTM zone 33N, Ell./Datum: WGS84.



### 2.3. EO and Sea Truth Data

One of the main goals of the methodology implemented in this work was to test the effective detection and mapping of the PO growing in the seabed within the euphotic zone, using sea truth and HR remote sensing airborne techniques in these middle Tyrrhenian areas where the previously described impact factors and turbidity are present. In this perspective the exploitation of the measurements acquired in the areas of interest during a sea truth campaign started in 2012 as calibration and test was pursued. Previously in 2011 a preventive inspection of PO meadows located along the coast of interest was conducted aiming at suitably selecting and positioning (by means of GPS techniques) all the measurement stations in order to be representative of the local PO effective distribution (Figure 2). Once defined the stations distribution the measurement phase started earlier focusing on the stations located in correspondence of the most endangered meadows in the more threatened sites (*i.e.*, ports, anchorages, touristic beach). The measurements included the usual plant biometric parameters (density, biomass, *etc.*) derived from suitable sampling schema based on a statistical approach involving partial measurements and samples gathering from 1 m<sup>2</sup> subplots (5–10), randomly distributed around (within a 15 m. radius) the station centre. Considering that even if these preliminary acquired sea truth measurements are not fully synchronous with Daedalus ATM flight, most of them refer to late summer PO meadow rest condition in the subsequent year and happened unchanged respect to previous inspection, so we assumed that they were usefully exploitable for calibration and validation purposes in this context. As you can see (Figure 1) in our area of interest the sampling stations measurements show a sufficient range of PO density values (Table 1). The preliminary evaluation of the results of sea truth measurements acquired on the PO meadows of Civitavecchia shallow waters during last 2 years until now, confirmed the above cited ecosystem stress factors especially around the harbors where there is a concentration of ship traffic and anthropic induced PO stress factors. In fact, as you can see in Table 1, the Civitavecchia PO phenology mean data referring to some important parameters like dry biomass and density happened lower than those acquired on the other coastal sites of S. Marinella (Figure 2, central Tyrrhenian coast) and Monterosso, located in Ligurian sea, in the Northern Tyrrhenian coast. Starting from these reflections and considering the capability of this airborne remote sensing system in terms of ground resolution and radiometry dynamic a Daedalus ATM 1268E strip was acquired on 23 October 2011 along the coastal area of interest (Figure 2) corresponding to harbors coastal shallow waters environment, and then its multispectral data, recoded under form of 16 bit digital count (DC), were exploited for methodology implementation. These multispectral data were acquired during a flight at 1000 m. height and with 2.5 m. of ground resolution (2.5 m/pixel). This airborne system is based on a 12 bit radiometry and 2.5 mrad IFOV (86° FOV) sensor integrated with a inertial unit in order to obtain automatic roll and S-bend geometrical distortions correction. Given the system availability temporal window, the flight was carried out on October at 08.30 in the morning with good weather and atmosphere transparency situation although the sun height and date weren't optimal for the sea bed imaging. In addition a 7 bands Landsat ETM+ (Enhanced Thematic Mapper plus) frame, acquired on 2 October 2011, during the same month of Daedalus flight was exploited to implement an efficient image based atmospheric correction step of ATM (Advanced Thematic Mapper) 1268E multispectral data based on the spectral



equivalence of some acquisition channel of sensors (see Table 2) to recover the so-called water leaving radiance/reflectance signal.

**Table 1.** Intercomparison between PO meadows phenology parameters derived from sea truth data acquired on Civitavecchia (8 stations) and other two different sites (about 10 stations) of the Tyrrhenian coast. The SD (Standard Deviation) values refer to stations number which is different for each site.

PO Meadows Site	n° Leaves $\pm$ SD	Width (cm) $\pm$ SD	Lenght (cm) $\pm$ SD	Biomass (Dry Weight) $\pm$ SD	Density n°Shoots/m <sup>2</sup> $\pm$ SD
Monterosso	6.32 $\pm$ 0.7	0.92 $\pm$ 0.11	53.57 $\pm$ 30.06	53.57 $\pm$ 30.06	259.72 $\pm$ 114.65
Civitavecchia	6.26 $\pm$ 1.3	0.95 $\pm$ 0.08	29.74 $\pm$ 17.15	29.74 $\pm$ 17.15	313.54 $\pm$ 114.21
S. Marinella	5.54 $\pm$ 0.6	0.99 $\pm$ 0.08	32.16 $\pm$ 7.32	32.16 $\pm$ 7.32	359.25 $\pm$ 106.22

Being interested on the useful reflectance signal coming from seagrass plants standing on the seabed it was further necessary to remove the noise contribution introduced by over standing water column [20,21]. To this end the assessment of the wavelength-dependent diffuse attenuation coefficient  $k_d$  distribution, obtained from MERIS (MEdium Resolution Imaging Spectrometer) satellite sensor, was introduced based on the same spectral equivalence concept (Table 2). These water column thematic products are implemented within a the recent Coastcolour project [16], funded by ESA (European Space Agency) to provide support specifically devoted to coastal, optically complexes, shallow waters monitoring applications. The main characteristic of coastal waters is that they are in general more optically complex (Case 2 waters) than the open ocean (Case 1 waters) and may present large optical gradients. Such strong optical gradients require further development and refinement of radiative transfer models, well established for ocean colour of open seas, taking into account the combined effect of higher concentration and number of the optically-active substances (chlorophyll, Gelbstoff, inorganic suspension, organic detritus) which often dominate coastal shallow waters. In turn, the bio-optical models so refined can be useful in open-ocean applications, where the optical gradients are often much more subtle. While the acquired data from MERIS, MODIS and SeaWiFS satellite sensors already support the OceanColor operative monitoring global services for open seas (Case 1 waters), the European Space Agency has launched the Coastcolour project to work towards these objectives by developing, demonstrating, validating and intercomparing different Case 2 algorithms over a global range of coastal water types found in different world areas including the entire Mediterranean sea (Figure 3). Coastcolour preoperative project will fully exploit the potential of the MERIS instrument for remote sensing of coastal zone water taking into account its spectral-spatial features including its increased monitoring capability in visible range (6 channels) coupled with a 300 m. of senso ground spatial resolution. A first set of Coastcolour products includes a revised Level 1 product and atmospherically corrected coastal products. The Level 1P product is a refined top of atmosphere radiance product compared with the standard MERIS Level 1b product. It provides improved geolocation and calibration, equalisation to reduce coherent noise, smile correction, pixel characterization information (cloud, snow, etc.), a precise coastline and a reformatting into standard format. The Level L2R product is the result of the atmospheric correction. It contains water leaving reflectance, normalised water leaving reflectance and different information about atmospheric

properties. The L2W product provides information about water properties such as IOPs, concentrations and other variables including the water diffuse attenuation coefficients in the wavelengths of interest which were used here. It also contains an ortho-corrected geo-coding and different flags characterizing pixels.

**Figure 3.** MERIS Coastcolour project test areas for coastal shallow waters characterization through coastal zone color satellite remote sensing and on purpose developed methods.

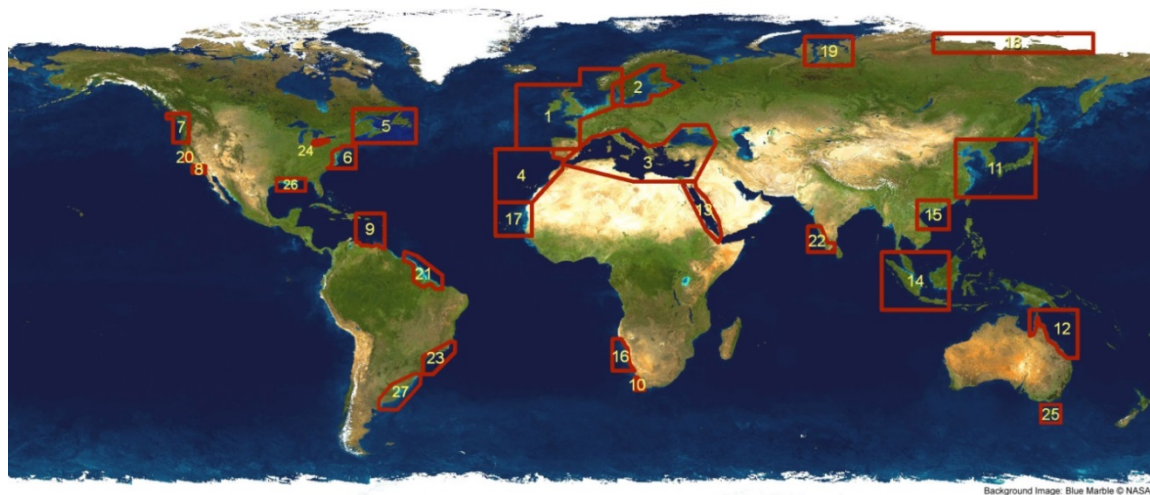


**Table 2.** Daedalus ATM HR spectral channels and related MERIS and ETM+ bands.

MERIS			Daedalus ATM 1268 E			Landsat ETM+		
Band	$\lambda_{\text{cent}}$ (nm)	$\Delta\lambda$	Band	$\lambda_{\text{cent}}$ (nm)	$\Delta\lambda$	Band	$\lambda_{\text{cent}}$ (nm)	$\Delta\lambda$
1	412.69	9.94						
2	442.56	9.95	1	435	30			
3	489.88	9.96	2	485	70	1	485	70
4	509.82	9.96						
5	559.69	9.97	3	560	80	2	560	80
6	619.60	9.98	4	615	20			
7	664.57	9.99	5	660	60	3	660	60
8	680.82	7.49						
9	708.33	9.99	6	722.5	55			
10	753.37	7.50						
12	778.41	15.01						
13	864.88	20.05	7	830	140	4	835	130
			8	980	140			
			9	1,650	200	5	1,650	200
			10	2,215	270	7	2,220	260
			12	10,750	4,500	6	11,450	2,100

#### 2.4. Preprocessing Daedalus ATM Multispectral Data

Due to operational restraints and lack of simultaneous water and atmosphere turbidity *in situ* measurements, the preprocessing methodology was implemented using the “image based” approach for atmospheric and water column) radiometric preprocessing. The “image based” approach exploits specific information contained in the same multispectral image to be corrected and do not require

additional *in situ* field measurements simultaneous to the satellite/aircraft overpass and furthermore being easy to apply is adapt for our operative use. In particular the recorded DC for the nonthermal channels of the 1268 E ATM sensor were converted to ground reflectance using the ELM (empirical line method) [22,23]. This method, used for satellite [24] and aircraft [25] remotely sensed multispectral data, correlates recorded band DC to known band reflectance values of surface targets (Figure 4). In such a way based on the assumption that within the image, there are at least two targets of low and high reflectance for the spectral bands of interest recorded by the ATM sensor it was possible to transform the recorded DC through a linear equation obtained from related best-fits models (Figure 5), to account for atmospheric effects. The higher spectral reflectances of the sand bar surfaces at various locations within the Civitavecchia corridor were considered both with dark objects consisting of areas with the lowest and most uniform digital values, such as shadowed areas. Other surfaces (e.g., dense, closed-canopy and tilled ground) with intermediate reflectance values in some of the ATM band wavelengths were also used in order to better define the linear regression between recorded ATM band DC values and ground reflectance derived from ETM+ sensor in the visible and NIR ranges. The observed digital numbers of the nonthermal ATM bands within such areas were consistent throughout the expected ranges. These ground reflectance values derived for each target area from atmospherically corrected ETM+ imagery acquired in the same month of the ATM 1268E flight, were suitably interpolated in order to match the Daedalus ATM bands (Table 2). The Landsat ETM+ data were exploited for Daedalus ATM atmospheric correction since the currently available correction packages are generally more able to handle remotely sensed data from this sensor for which there are also available corrected reflectance image data in the official repositories. In fact our orthorectified ETM+ reference frame was previously atmospherically corrected to recover ground reflectances using a commercial code (FLAASH) able to remove also the adjacency noise effects. In the subsequent step the ETM+ ground reflectances of the above described target points were recorded both with correspondent DC values derived mainly from land features and surfaces encompassed within the geometrically corrected Daedalus ATM strip.

**Figure 4.** Point target (P1–P10) ground spectral signatures applied with ELM method. The dash-contoured x-labels indicate the ETM+ reflective bands correspondence.

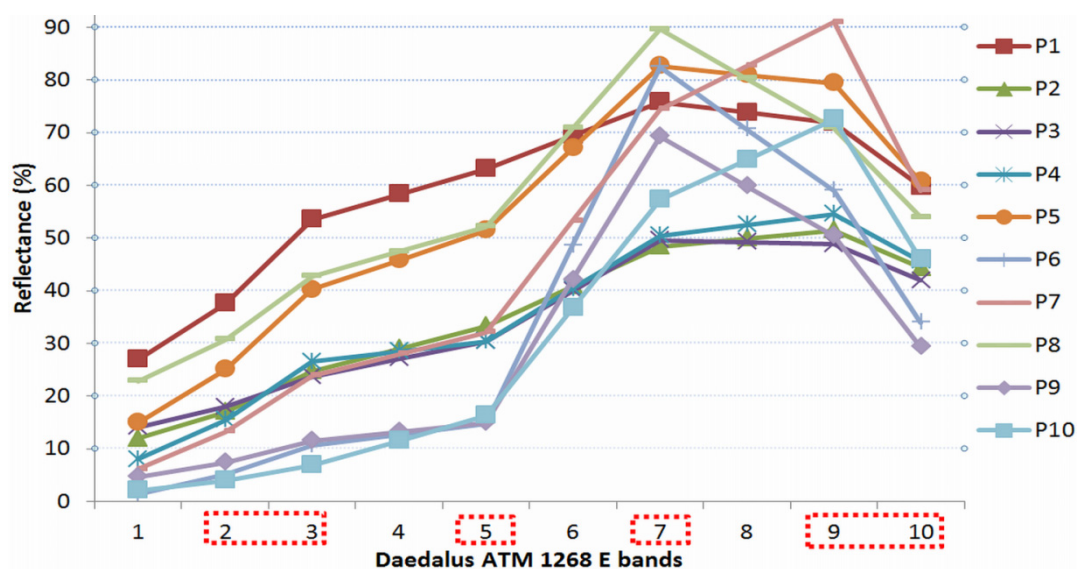
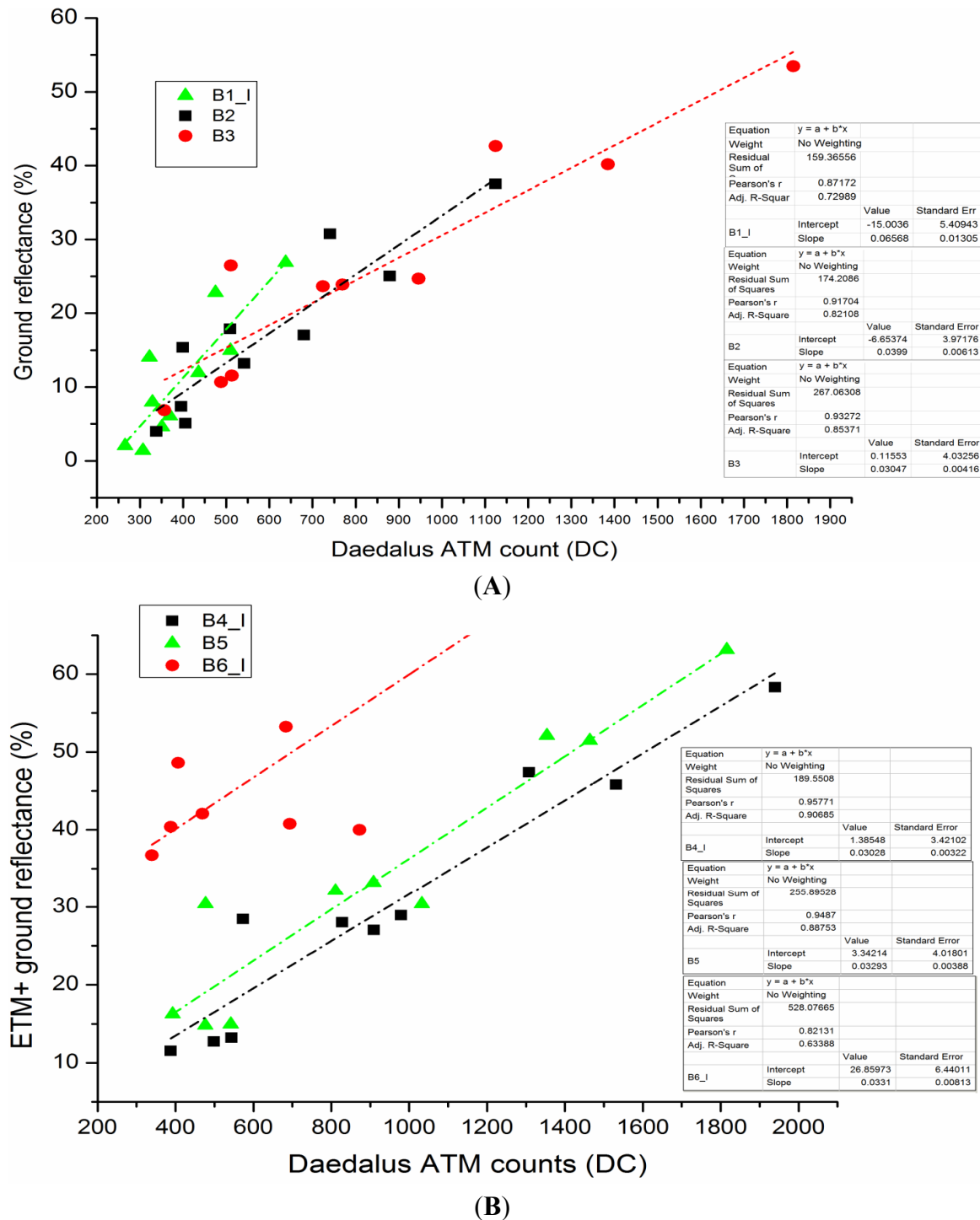


**Figure 5.** Regression models for Daedalus ATM reflectance ground retrieval through ELM method from ETM+ atmospherically corrected ground reflectance data for bands 1–3 (A) and bands 4–6 (B). Here BX state for the related Daedalus spectral band while the I suffix means interpolated data.



In this way a linear regression model was derived for each Daedalus ATM bands in order to retrieve the corresponding ground reflectance map to be further processed for water column noise accounting. As you can see in Figure 5, the ELM regression models for the first six Daedalus ATM bands in the visible and NIR wavelengths, the most important for the coastal ecosystems monitoring, look very

good since their correlation coefficients are between 0.67 (band 6 at 722.5 nm) and 0.92 (band 4 at 615 nm) and the related F-values remain lower than  $10^{-4}$ . Due to interpolation issues the calculated reflectance in band 1 (BI\_I points set in right graph of Figure 5) shows negative values for 2 target points which are rescaled within the 100% physical range and the related model remains enough consistent ( $R^2 = 0.76$ , F-value  $< 10^{-4}$ ).

Remote sensing of the seagrass growing in sea bed, respect to terrestrial applications for vegetation monitoring, shows additional limiting factors concerning the perturbing effects introduced by coastal water column to reflectance/radiance  $R_{bi}$  useful signals [20,24] coming from vegetation in sea bottom and acquired by remote sensors. The water column not only attenuates these useful reflectance signals but introduces also its own specific spectral components dependent on the concentration of the optically active constituents and on its depth [26,27].

This cumulative effect may be at first order approximately described using the wavelength dependent water attenuation coefficient,  $k_{di}$  [ $m^{-1}$ ] in the following formulation [17]:

$$R_{oi} = R_{wi} + (R_{bi} - R_{wi}) e^{-2K_{di}Z} \quad (1)$$

where:

$R_{oi}$  = radiance/reflectance (atmospherically corrected) at water surface;

$R_{wi}$  = radiance/reflectance corresponding to extinction water depth;

$k_{di}$  = light diffuse sea water attenuation wavelength-dependent coefficient;

$R_{bi}$  = radiance/reflectance from the sea bed;

$Z$  = water depth (bathymetry);

$i,j$  = spectral index (*i.e.*, acquisition band number).

According to Lyzenga semi empiric method a two bands ( $i,j$ ) reflectance ratios (logarithmic differences) of logarithmic expressions of equation 1 may be used to assess a bathymetry-independent seabed reflectance index SBRI:

$$SBRI_{ij} = \log (R_{oi} - R_{wi}) - (k_{di}/k_{dj}) \log (R_{oj} - R_{wj}) \quad (2)$$

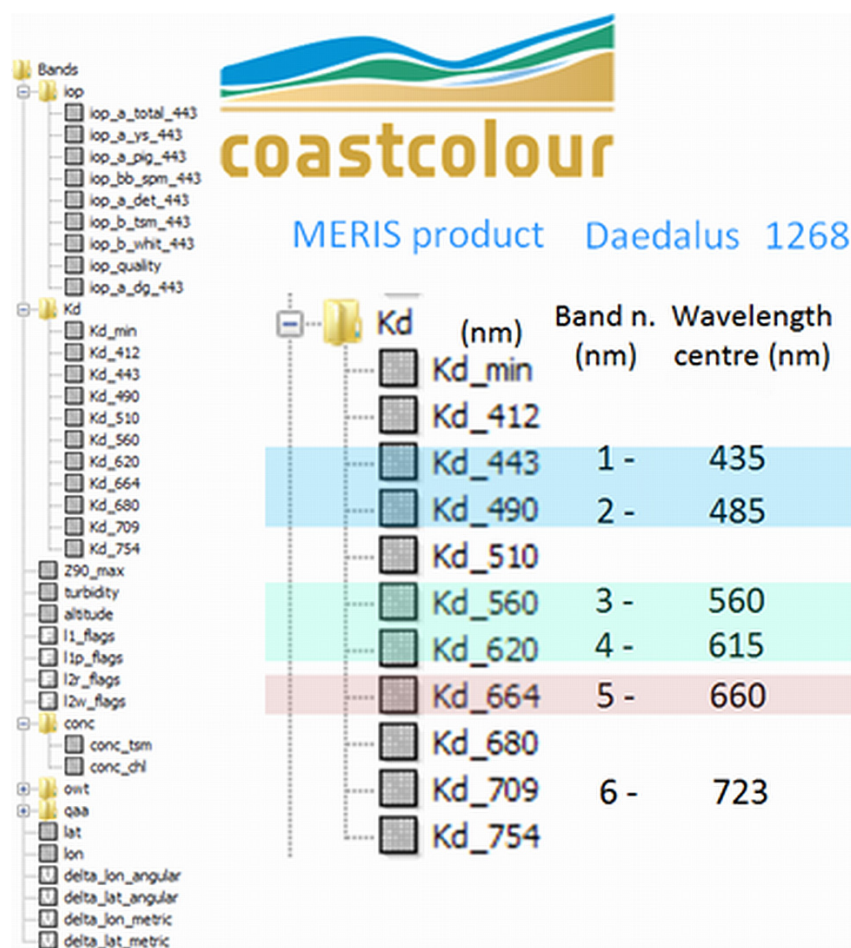
where the water column optical effects are reduced. Thus from estimated  $k_{di}$  for each ratio of two acquisition bands it is possible to obtain a water column corrected SBRI index, only dependent on the seabed reflectance properties related to different substrates and seagrass. In such a way it is possible without bathymetric data to exploit this “image based” approach based on the Lyzenga [28] algorithm which utilizes two spectral reflectance ratio ( $R_{oi}/R_{oj}$ ) to obtain a water depth independent index SBRI on which may be based the discrimination and monitoring of the various seagrass on the seabed.

In our approach, to account for the spatial variability of each  $k_{di}$  in coastal shallow water environment, their assessed distributions obtained from MERIS Coastcolour products, compatible in terms of acquisition bands (Figure 6) and time with Daedalus ATM data, were interpolated over the area of interest in order to homogenize their ground resolution.

Finally, according to relationship 2, the SBRI maps corresponding to various ratios mainly in the visible ranges, were produced using these Coastcolour derived  $k_{di}/k_{dj}$  distributions, the atmospherically corrected reflectance  $R_{oi}$  and  $R_{wi}$  extinction reflectance mean values estimated from preprocessed Daedalus ATM imagery. Considering the more relevant effectiveness of visible light in sea water penetration the preprocessed Daedalus ATM multispectral ground/water reflectance data were utilized

to obtain the following five seabed Lyzenga reflectance index layers using Equation (2):  $SBRI_{3,1}$ ,  $SBRI_{3,2}$ ,  $SBRI_{4,3}$ ,  $SBRI_{5,2}$ ,  $SBRI_{6,3}$ , where the subscript indices state for the Daedalus ATM band number in the visible and NIR ranges as reported in Table 2. All these layers are then stitched in a multispectral raster file in order to allow the subsequent classification/clustering step.

**Figure 6.** Coastcolour MERIS thematic products included the  $K_d$  coefficients corresponding to Daedalus ATM 1268E bands (within the colored strips).



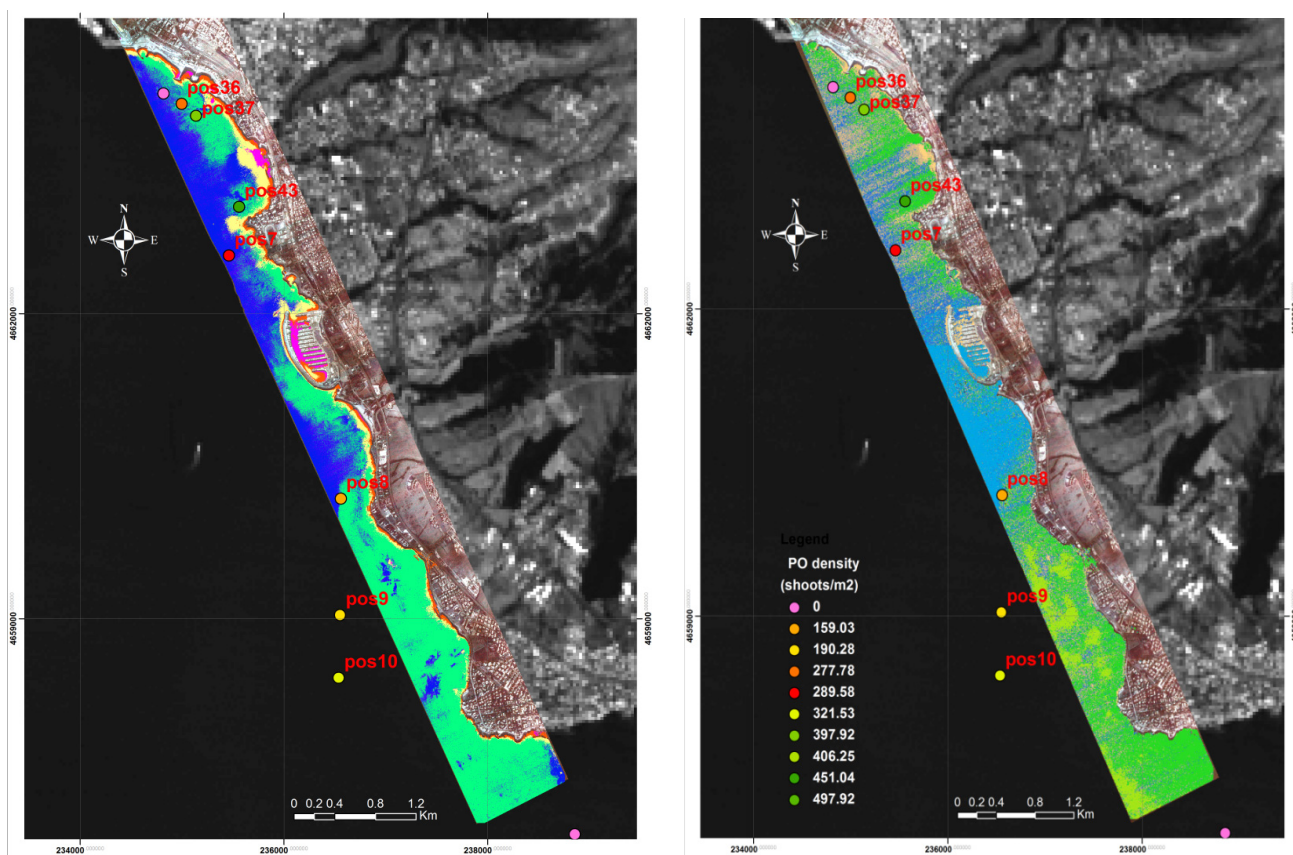
## 2.5. Thematic Mapping and Classification

The primary goal of the current work was to evaluate the Daedalus ATM 1268E airborne system mapping capability of coastal ecosystems and radiometric preprocessing of its multispectral data based on operative “image based” approach, in particular the above described Lyzenga method. With this perspective first of all the synoptic distribution of PO and sea bottom classes was assessed starting from pre-processed (geometrically and atmospherically corrected) Daedalus ATM multispectral data by means of the SAM (Spectral Angle Mapper) statistical classification scheme [29] and using the spectral signatures provided by previous ISODATA unsupervised algorithm. These formers were labeled by means of photointerpretation approach according to preexisting rough information about the local PO distribution. The same approach was applied for processing the multilayer file composed by the five above referenced Lyzenga’s spectral indices obtained from the equation 2 in order to reduce the sea water column effects on the water leaving useful reflectance signals.



The results obtained from the two procedures in term of thematic maps show very fragmented distributions characterized by different local densities of PO green pixels as displayed in Figure 7. Here you can see that we couldn't find more than one PO class using the corrected Daedalus ATM data while five Lyzenga's indices allowed to retrieve diverse PO types (different green shades in the right picture of Figure 7).

**Figure 7.** Thematic maps of PO distribution (green shades) along the Civitavecchia coast obtained by means of SAM classification of atmospherically corrected Daedalus ATM 1268E (**Left**) strip data and of derived Lyzenga's SBRI five indices (**Right**). The PO sampling station point density (shoot/m<sup>2</sup>) classes are reported in overlay as colored dots representing local PO density while a ETM+ band 4 was used as gray shades background. Cartographic Projection: UTM zone 33N, Ell./Datum: WGS84.



The PO classified cover density (n° of classified PO pixel/m<sup>2</sup>) from the classification maps seem to agree with the point measurements density (shoots/m<sup>2</sup>) of the sampling station located within the strip area, since the lower density ones (red-yellow) are located outside or at borders of most dense green PO zones obtained by means of SAM classification of atmospherically corrected Daedalus ATM 1268E (left) strip data and of derived Lyzenga's SBRI five indices (right). The PO sampling station point density (shoot/m<sup>2</sup>) classes are reported in overlay as colored dots representing local PO density while a ETM+ band 4 was used as gray shades background.

Although in general the two distributions look similar they differ in some areas and particularly in correspondence of pos37 sampling station and near the touristic harbor where we found much less dense PO meadows with Lyzenga's approach.

### 3. Results and Discussion

Due to lack of reliable preexisting PO maps and because of type (the acquisition refers to PO meadow continuous variables while the classification maps deal with categorical binary variables) and scarcity of sea truth measurement stations (only five) on the sea strip area it was impossible to test the previous EO-derived thematic maps accuracy using the usual methods (random samples, confusion matrix, k statistic). Given these limitations to this end an original approach based on the available point measurements from the five sampling stations was implemented. In particular, considering that, due to evident local PO meadows fragmentation, the per pixel classification results are enough scattered (salt and pepper effects), classified PO density (in terms of percentage of PO classified pixels) could be retained assimilable to local PO meadow % coverage directly linked to measured LAI distribution within the different neighborhood areas of each sampling station.

Therefore such classified PO point density values were assessed from SAM classification result (Figure 7), using a GIS focal analysis algorithm with different focal square windows (sizes: 9, 15, 25 pixels) compatibles with sea truth sampling schema. In Figure 8 the PO density and related LAI measured at five sampling stations were reported with the corresponding focal densities derived using different windows (15, 25) from classification maps obtained respectively from atmospherically corrected Daedalus ATM reflectances and Lyzenga indices. These so assessed PO focal density (classified) local values obtained from the two classification products (Figure 7) in the five stations were compared with the related point LAI values derived from sea truth point station measurements. In such a way, through regressive models ( $LAI = a * X + b$ , where the independent variable X state for the above cited focal PO densities derived from the classified maps), we were able to test the agreement of two thematic maps with the sea truth point measurements in term of correlation level ( $R^2$ ). In Table 3 there are reported the regression coefficients (a, b) and the relative statistical parameters including the coefficient of determination ( $R^2$ ) of models using the PO densities obtained from classifications of Daedalus ATM atmospherically corrected responses (DExx code) and of related Lyzenga's indices (LYxx code). These PO densities were assessed on three different neighborhood window (the window size in square pixels is indicated by the two digit suffix xx of the code) around the reference sampling station location. As you can see in general the density values derived from both (DE & LY) classification maps well agree with the measured LAI at different neighborhood windows sizes with correlation ranging between 0.61 and 0.839  $R^2$  and 0.118 for the worst F-value. The best  $R^2$  is related to Lyzenga's indices classification and LY25 code whose linear model coefficients and statistical parameters are shown in Table 4. Here in particular the adjusted  $R^2$  of 0.786 and regression S. Error of 0.539 confirm the goodness of the assessed model:  $LAI = 3.6527 LY25 - 0.98$ , where the leaf area index (LAI) distribution of PO patch is expressed in terms of mean density of PO classified pixels (LY25) obtained from Lyzenga's indices within a  $25 \times 25$  pixels square window as independent variable. As you can see in Table 3 the LYxx models show a correlation increases with focal window size while  $R^2$  is decreasing for DE15 obtained through a focal window size (~562 m) lower than that adopted for sampling area (~706 m) for assessing the sea truth measurement at station level.

**Figure 8.** LAI and PO density (shoots/m<sup>2</sup>) rescaled point measurements and corresponding corver focal densities derived from classification of Daedalus ATM reflectances (DExx) and Lyzenga indices (LYxx).

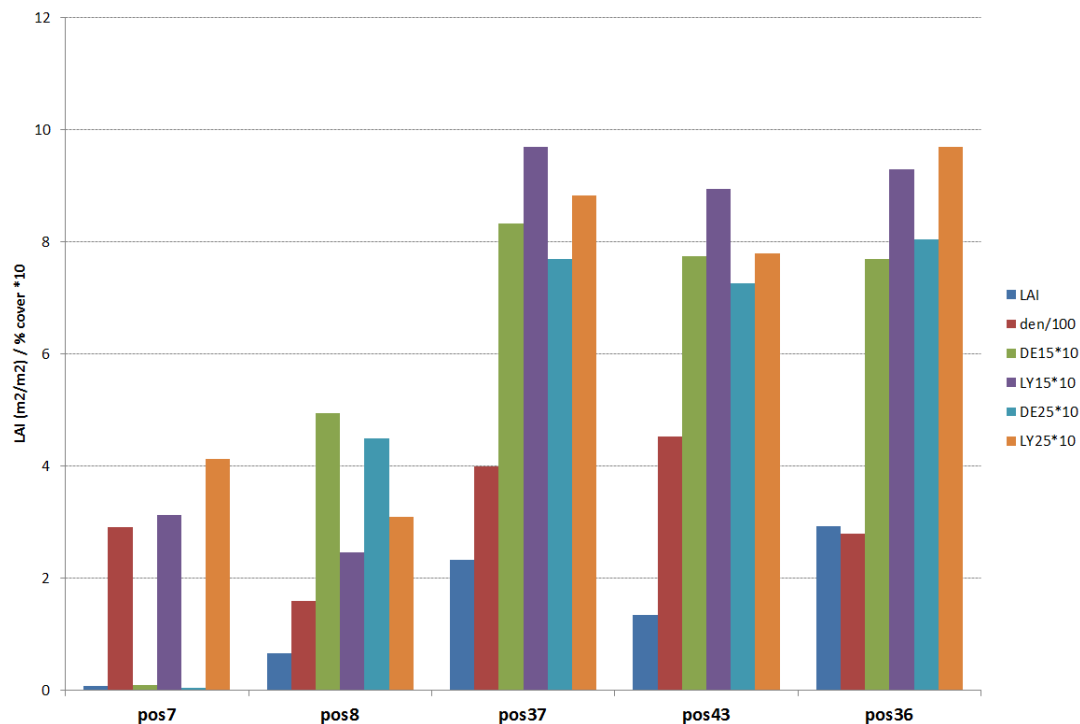


**Table 3.** LAI modeling through Daedalus ATM (DExx) reflectances and Lyzenga indices (LYxx) using different neighoohd window sizes around the sampling stations centre.

	LAI (m <sup>2</sup> /m <sup>2</sup> )			
	a	b	R <sup>2</sup>	F-value
DE9	21.91	−0.203	0.75	0.057
DE15	2.824	−0.165	0.687	0.082
DE25	3.04	−0.211	0.765	0.051
LY9	17.12	0.061	0.61	0.118
LY15	2.803	−0.417	0.744	0.059
LY25	3.652	−0.987	0.839	0.028

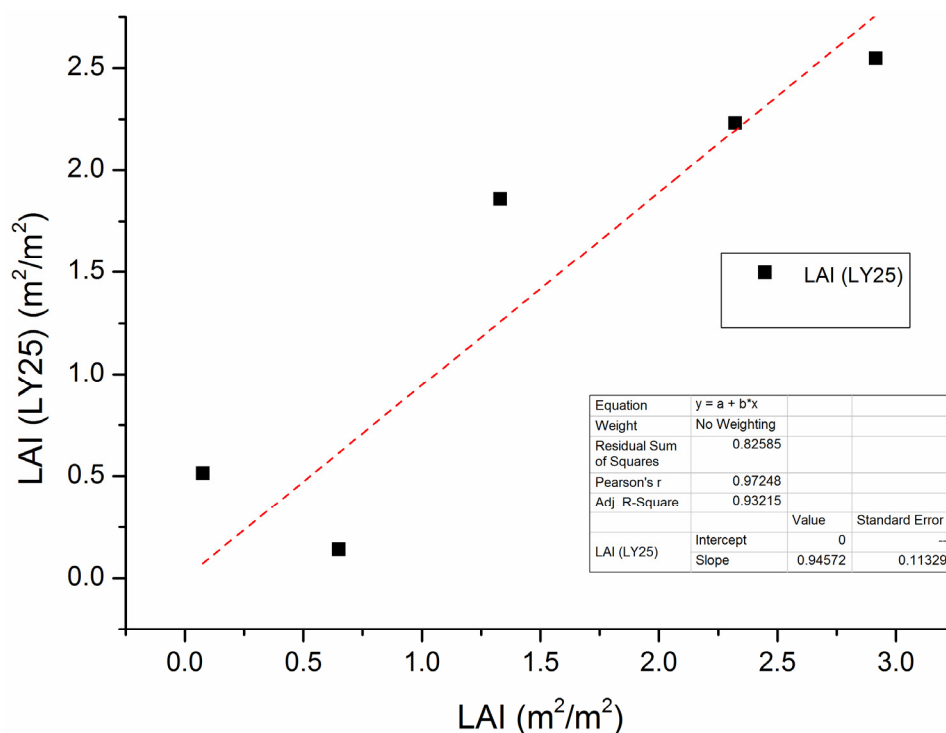
**Table 4.** LY25 model coefficients and related statistical parameters.

	Coefficient	Std. Error	t-ratio	p-value
const	−0.9878	0.6625	−1.4909	0.2328
LY25	3.6527	0.9213	3.9648	0.0287
Mean dependent var	1.4587	S.D. dependent var		1.1671
Sum squared resid	0.8733	S.E. of regression		0.5395
R-squared	0.8397	Adjusted R-squared		0.7863
F(1, 3)	1.5719	P-value(F)		0.0287
Log-likelihood	−2.7323	Akaike criterion		9.4646
Schwarz criterion	8.6834	Hannan-Quinn		7.368107

In any case, despite the adverse result obtained with the smallest focal window (LY9) which, due to its size, too reduced respect that of sea truth, is less representative, the bigger  $R^2$  values referring to LY15 and LY25 models respect to corresponding DE15 and DE25 may be considered a preliminary indication about the effectiveness of Lyzenga method to reduce water column effect.

In Figure 9 the LAI values obtained from the sea truth point data referring to five sampling stations vs. the corresponding modeled results obtained from LY25 focal desities were displayed. Here you can see the significative agreement ( $R_{adj}^2 = 0.93$ ) between the measured and corresponding modeled LAI values which gives a favorable indication about the capability of the Daedalus ATM derived Lyzenga reflectance indices for seagrass and seabed monitoring in turbid shallow waters.

**Figure 9.** Measured (x-axis) vs. modeled (y-axis) LAI using the LY25 model coefficients.



In general, sea truth acquisition refers to *in situ* areal measurement of continuous biophysical variables (shoots density, leaf number per shoot, leaf area, % coverage, LAI, ...) which aren't easily usable for accuracy assessment of thematic maps, containing the binary distributions of categorical variables, without previous thresholds definition for presence/absence of target classes. In the implemented procedure a continuous variable (PO focal density) was derived from thematic one (PO distribution) in order to allow the agreement evaluation with LAI point data acquired at measurement station level. The different PO distribution (in term of presence/absence, binary on/off categorical variable) from two thematic maps obtained from the classification of Daedalus ATM atmospherically preprocessed data with and without water column, were processed by means of focal analysis to derive the local PO class focal density, continuous variable point values. These values were extracted in correspondence of the sea truth station locations characterized mostly by fragmented PO class using different kernel sizes to try to account for the sampling area circular shape and the spatial quantization of remote sensing data. Then an usual statistic OLS (Ordinary Least Squares) regressive modeling

approach was exploited to assess their quantitative agreement in term of correlation with available sea truth data. In such a way it was possible to implement an original method, assimilable to accuracy assessment, applicable to the above cited maps through correlation estimates, without the above cited thresholding problematic steps. From these preliminaries results and despite the unfavorable flight time (08.30) and date, first of all the general suitability of the Daedalus ATM 1268E airborne sensor for coastal ecosystems monitoring and specifically for PO mapping purposes must be outlined considering its spatial and radiometric resolution, spectral features and on flight geometric automatic correction for ATM 1268 E (Enhanced) platform capability. In addition, thanks to these sensor basic radiometric and geometric features it was possible to implement an effective “image based” two step radiometric preprocessing procedure for atmospheric and water column noise attenuation using respectively the ELM (Empirical Line Method) and the Lyzenga methods which improved the PO meadow detection and mapping in the turbid shallow waters near to harbors of Civitavecchia town.

To evidence and quantify these enhancements two different PO distributions (Figure 7) within area of interest were produced from the data preprocessed at the two different levels by means the same statistical classification schema including the ISODATA and SAM algorithms. This former classification algorithm was selected since it performed the best within those preliminarily tested. Although both the produced maps show enough fragmented PO distribution (different green point density in two maps of Figure 7) within the most threatened meadows in correspondence of the central part of acquired strip, that derived from the Lyzenga’s indices rightly detect less dense PO distribution near the touristic harbor and different (light green shade) PO meadows (matte) in the lower part of the Daedalus strip. Finally, using an original procedure the two maps were tested on the basis of the point sea truth data previously acquired on the area of interest by comparing the measured LAI with the local PO density derived from the two classification maps within different focal windows located in correspondence of the related sea truth measurement stations. The LAI, in terms of leaf surface density distribution derived from the PO phenology measured data at meadow level (shoots density, mean leaf number per shoot, mean leaf width and length), like for the terrestrial vegetation represents one of main parameters determining the plant interaction with environment, in particular with electromagnetic radiation irradiated by the sun. Thus its correlation with the multispectral reflectance responses detected by Daedalus ATM 1268E sensor and derived products (Lyzenga’s indices, classification thematic maps) may be usefully exploited in this context like in the more widely diffused terrestrial application for vegetation monitoring. These preliminaries results, even if obtained through a limited sea truth data set, highlight the general agreement between the point measurement of LAI and the PO pixel density derived from the two classification maps ( $\min R^2 = 0.61$ ) with different focal windows (Table 3). The Lyzenga LY15 and LY25 models produced the highest correlation between the PO meadows LAI distribution around the assessed sampling stations and related focal PO density derived from classification products, and preliminarily confirmed in this context the efficacy of the adopted Lyzenga water column “image based” radiometric noise reduction approach. It should be further outlined that the suitable integration of the Landsat ETM+ for atmospheric correction and MERIS Coastcolour experimental products for water column noise reduction based on the spectral acquisition band equivalence, allowed us to exploit the synergy between these multi-resolution multispectral data and products to improve the operative HR remote sensing monitoring procedures of PO ecosystems in turbid shallow waters of Tyrrhenian coast.

In this context the choice of the ELM method for atmospheric correction was pursued taking into account its suitability to be routinely and efficiently (possibility to retrieve enough and suitable target points even not time invariants) used according to the above cited specific application needs and based on a preventive evaluation of alternative image based schemas, like those based on the pseudoinvariant target or dark objects approach [30].

#### 4. Conclusion

The general objective of this work was to check and assess the capability of Daedalus ATM 1268 E airborne remote sensing system for operative mapping and monitoring of the threatened and fragmented PO (*Posidonia Oceanica*) meadows in turbid shallow waters. It relies on general demand to improve the current method to gather effective and extensive information about these seagrass ecosystems using the most recent HR (High Resolution) remote sensing techniques especially in case of most threatened meadows in shallow and turbid waters. In this context the main constraints aroused from the specific application needs in terms of its operativity and from the kind and availability of sea truth data for calibration and validation purposes. In addition to sensors performance and a proper atmospheric noise removal, the effective remote mapping capability of the PO extents requires also a suitable water column radiometric preprocessing to account for possible signal attenuation by water turbidity which represents one of the most limiting factors for wider exploitation of HR remote sensing techniques in seagrass monitoring, especially in northern Mediterranean sea. To this end an innovative solution, based on image-based Lyzenga method, was developed here by coupling its intrinsic easy and operative applicability with improved accuracy derived from exploitation of wavelength dependent  $k_d$  (water diffuse attenuation coefficient) distributions, suitably derived from MERIS (Medium Resolution Imaging Spectrometer) data for coastal shallow waters of interest. The effectiveness of this preprocessing procedure was then assessed by means of an original benchmark test using two different thematic maps obtained from the same classification procedure of the atmospherically corrected Daedalus reflectance data at two different preprocessing levels (with and without water column correction) and the available sea truth point measurements. The implemented method for thematic accuracy assessing in term of correlation by means of focal analysis/regressive modeling and the *in situ* measurements, may be retained another important result applicable in case of availability of usual sea truth measurements (non specifically devoted to accuracy assessment) and fragmented classes arising from spectral per pixel classification procedures. It should be outlined that the usual sea truth data in general refer to continuous variable mean values within a sampling area around the measurement station centre which is larger than a single pixel of associated HR (High Resolution) imagery. On the other hand the *in situ* data for usual thematic accuracy assessment requires different measurements of binary categorical variables (presence/absence of reference class) at pixel level according to selected sampling schema, so it isn't possible to easily exploit to this end the previous sea truth acquisitions. In this framework the developed methodology not only gives a proper answer to the work general goals but also provides a useful and original solution for thematic accuracy evaluation using the common sea truth data, optimizing in such a way the exploitation of the expensive *in situ* acquisitions.



Although the obtained results seem encouraging, the water column preprocessing step might represent a critical aspect in term of compatibility of MERIS Coastcolour data which should be carefully evaluated and selected to be suitably representative of the water turbidity condition at moment of the HR remote sensing data acquisition.

The current perspectives of the above described research activities include new campaigns for acquiring additional measures of biophysical parameters corresponding to an increased station number along larger coastal areas of interest. The PO phenology seasonal trend will be considered according to synchronization of airborne Daedalus ATM acquisitions to be planned within more suitable time and date for sun height. In such framework the most recent satellite sensors (Landsat 8 OLI, Sentinel) data integration will be tested in order to improve the spatial coverage of the available multispectral imagery to be exploited for PO and other seagrass monitoring in this Tyrrhenian coast.

The overall goal is to further improve and validate the above presented methodology using both additional remotely sensed HR data and ampler sea truth data sets obtained from the ongoing measurement campaigns carried out over larger areas including different types of shallow waters turbidity, PO meadows and substrates.

## Acknowledgments

This work was partly carried out in the framework of RITMARE nationally funded project.

The authors gratefully acknowledge the “3° Reparto Capitanerie di Porto (Comando Generale del Corpo delle Capitanerie di Porto)” for the acquisition and providing of the Daedalus ATM 1268E imagery and in addition they wish to thank the “Direzione Marittima di Civitavecchia” for its general support to this work.

## Conflicts of Interest

The authors declare no conflict of interest.

## References

1. Marbà, N.; Duarte, C.M.; Cebrià, J.; Gallegos, M.E.; Olesen, B.; Sand-Jensen, K. Growth and population dynamics of *Posidonia oceanica* on the Spanish Mediterranean coast: Elucidating seagrass decline. *Mar. Ecol. Prog. Ser.* **1996**, *137*, 203–213.
2. Orth, R.J.; Carruthers, T.J.B.; Dennison, W.C.; Duarte, C.M.; Fourqurean, J.W.; Heck, K.L., Jr.; Hughes, A.R.; Kendrick, G.A.; Kenworthy, W.J.; Olyarnik, S.; *et al.* Global crisis for seagrass ecosystems. *BioScience* **2006**, *56*, 987–996.
3. Micheli, C.; Cupido, R.; Lombardi, C.; Belmonte, A.; Peirano, A. Changes in genetic structure of *posidonia oceanica* at monterosso al Mare (Ligurian Sea) and its resilience over a decade (1998–2009). *Environ. Manage.* **2012**, *50*, 598–606.
4. Rotini, A.; Belmonte, A.; Barrote, I.; Micheli, C.; Peirano, A.; Santos, R.O.; Silva, J.; Migliore, L. Effectiveness and consistency of a suite of descriptors for assessing the ecological status of seagrass meadows (*Posidonia oceanica* L. Delile). *Estuar. Coast. Shelf Sci.* **2013**, *130*, 252–259.

5. Micheli, C.; Borfecchia, F.; De Cecco, L.; Martini, S.; Ceriola, G.; Bollanos, S.; Vlachopoulos, G.; Valiante, L.M.; Fresi, E.; Campbell, G. Seagrass monitoring by remote sensing in the context of biodiversity conservation. *Rapp. Comm. Int. Mer. Médit.* **2010**, *39*, 778–779.
6. Phinn, S.; Roelfsem, C.; Dekker, A.; Brando, V.; Anstee, J. Mapping seagrass species, cover and biomass in shallow waters: An assessment of satellite multi-spectral and airborne hyper-spectral imaging systems in Moreton Bay (Australia). *Remote Sens. Environ.* **2008**, *112*, 3413–3425.
7. Wabnitz, C.C.; Andréfouët, S.; Torres-Pulliza, D.; Müller-Karger, F.E.; Kramer, P.A. Regional-scale seagrass habitat mapping in the Wider Caribbean region using Landsat sensors: Applications to conservation and ecology. *Remote Sens. Environ.* **2008**, *112*, 3455–3467.
8. Klemas, V. Airborne remote sensing of coastal features and processes: An overview. *J. Coast. Res.* **2013**, *29*, 239–255.
9. Rainey, M.P.; Tyler, A.N.; Gilvear, D.J.; Bryant, R.G.; McDonald, P. Mapping intertidal estuarine sediment grain size distributions through airborne remote sensing. *Remote Sens. Environ.* **2003**, *86*, 480–490.
10. Brown, K. Increasing classification accuracy of coastal habitats using integrated airborne remote sensing. *EARSeL eProc.* **2004**, *3*, 34–42.
11. Pasqualini, V.; Pergent-Martini, C.; Pergent, G.; Agreil, M.; Skoufas, G.; Sourbes, L.; Tsirika, A. Use of SPOT 5 for mapping seagrasses: An application to *Posidonia oceanica*. *Remote Sens. Environ.* **2005**, *94*, 39–45.
12. Lyons, M.; Phinn, S.; Roelfsema, C. Integrating Quickbird multi-spectral satellite and field data: Mapping bathymetry, seagrass cover, seagrass species and change in Moreton Bay, Australia in 2004 and 2007. *Remote Sens.* **2011**, *3*, 42–64.
13. Ferrari, B.; Raventos, N.; Planes, S. Assessing effects of fishing prohibition on *Posidonia oceanica* seagrass meadows in the Marine Natural Reserve of Cerbère-Banyuls. *Aquat. Bot.* **2008**, *8*, 295–302.
14. Fornes, A.; Basterretxea, G.; Orfila, A.; Jordi, A.; Alvarez, A.; Tintore, J. Mapping *Posidonia oceanica* from IKONOS. *ISPRS J. Photogram. Remote Sens.* **2006**, *60*, 315–322.
15. Collin, A.; Archambault, P.; Planes, S. Bridging ridge-to-reef patches: Seamless classification of the coast using Very High Resolution Satellite. *Remote Sens.* **2013**, *5*, 3583–3610.
16. Ruddick, K.; Brockmann, C.; Doerffer, R.; Lee, Z.; Brotas, V.; Fomferra, N.; Groom, S.; Krasemann, H.; Martinez-Vicente, V.; Sa, C.; *et al.* The COASTCOLOUR project regional algorithm round Robin exercise. *Proc. SPIE* **2010**, 7858, doi:10.1117/12.869506.
17. Dekker, A.G.; Brando, V.E.; Anstee, J.M. Retrospective seagrass change detection in a shallow coastal tidal Australian lake. *Remote Sens. Environ.* **2005**, *97*, 415–33.
18. Chavez, P.S. Jr. Image-Based Atmospheric Corrections Revisited and Improved. *Photogram. Eng. Remote Sens.* **1996**, *62*, 1025–1036.
19. Wu, J.; Wang, D.; Bauer, M.E. Image-based atmospheric correction of quick-bird imagery of minnesota cropland. *Remote Sens. Environ.* **2005**, *99*, 315–325.
20. Borfecchia, F.; De Cecco, L.; Martini, S.; Ceriola, G.; Bollanos, S.; Vlachopoulos, G.; Valiante, L.M.; Belmonte, A.; Micheli, C. *Posidonia oceanica* genetic and biometry mapping through HR satellite spectral vegetation indices and sea truth calibration. *Int. J. Remote Sens.* **2013**, *34*, 4680–4701.

21. Mumby, P.J.; Clark, C.D.; Green, E.P.; Edwards, A.J. Benefits of water column correction and contextual editing for mapping coral reefs. *Int. J. Remote Sens.* **1998**, *19*, 203–210.
22. Moran, M.S.; Bryant, R.; Thome, K.; Ni, W.; Nouvellon, Y.; Gonzalez-Dugo, M.P.; Qi, J.; Clarke, T.R. A refined empirical line approach for reflectance factor retrieval from Landsat5 TM and Landsat7 ETM+. *Remote Sens. Environ.* **2001**, *78*, 71–82.
23. Palubinskas, G.; Müller, R.; Reinartz, P.; Schroeder, M. Radiometric normalization of sensor scan angle effects in optical remote sensing imagery. *Int. J. Remote Sens.* **2007**, *28*, 4453–4469.
24. Karpouzli, E.; Malthus, T. The empirical line method for the atmospheric correction of IKONOS imagery. *Int. J. Remote Sens.* **2003**, *24*, 1143–1150.
25. Hadley, C.B.; Garcia-Quijano, M.; Jensen, J.R. Empirical vs. Model-based atmospheric correction of digital airborne imaging spectrometer hyperspectral data. *Geocarto. Int.* **2005**, *4*, 21–28.
26. Mishra, D.R.; Narumalani, S.; Rundquist, D.; Lawson, M. Characterizing the vertical diffuse attenuation coefficient for downwelling irradiance in coastal waters: Implications for water penetration by high resolution satellite data. *ISPRS J. Photogram. Remote Sens.* **2005**, *60*, 48–64.
27. Bierwirth, P.N.; Lee, T.J.; Burne, R.V. Shallow sea floor reflectance and water depth derived by unmixing multispectral imagery. *Photogram. Eng. Remote Sens.* **1993**, *59*, 331–338.
28. Pahlevan, N.; Valadanzou, M.J.; Alimohamadi, A. A Quantitative Comparison to Water Column Correction Techniques for Benthic Mapping Using High Spatial Resolution Data. In Proceedings of ISPRS Commission VII Mid-Term Symposium on Remote Sensing: From Pixels to Processes, Enschede, The Netherlands, 8–11 May 2006.
29. Kruse, F.; Lefkoff, A.B.; Boardman, J.W.; Heidebrecht, K.B.; Shapiro, A.T.; Barloon, P.J.; Goetz, A. The spectral image processing system (SIPS)—Interactive visualization and analysis of imaging spectrometer data. *Remote Sens. Environ.* **1993**, *44*, 145–163.
30. Maas, S.J.; Rajan, N. Normalizing and converting image DC data using scatter plot matching. *Remote Sens.* **2010**, *2*, 1644–1661.